Cell Death and Differentiation (2014) 21, 1185–1197

www.nature.com/cdd

Novel signaling axis for ROS generation during K-Ras-induced cellular transformation

M-T Park[1,2,5], M-J Kim[1,3,5], Y Suh[1,5], R-K Kim[1], H Kim[1], E-J Lim[1], K-C Yoo[1], G-H Lee[1], Y-H Kim[1], S-G Hwang[4], J-M Yi[2] and S-J Lee*[,1]

Reactive oxygen species (ROS) are well known to be involved in oncogene-mediated cellular transformation. However, the regulatory mechanisms underlying ROS generation in oncogene-transformed cells are unclear. In the present study, we found that oncogenic K-Ras induces ROS generation through activation of NADPH oxidase 1 (NOX1), which is a critical regulator for the K-Ras-induced cellular transformation. NOX1 was activated by K-Ras-dependent translocation of $p47^{phox}$, a subunit of NOX1 to plasma membrane. Of note, PKCδ, when it was activated by PDPK1, directly bound to the SH3-N domain of $p47^{phox}$ and catalyzed the phosphorylation on Ser348 and Ser473 residues of $p47^{phox}$ C-terminal in a K-Ras-dependent manner, finally leading to its membrane translocation. Notably, oncogenic K-Ras activated all MAPKs (JNK, ERK and p38); however, only p38 was involved in $p47^{phox}$-NOX1-dependent ROS generation and consequent transformation. Importantly, K-Ras-induced activation of p38 led to an activation of PDPK1, which then signals through PKCδ, $p47^{phox}$ and NOX1. In agreement with the mechanism, inhibition of p38, PDPK1, PKCδ, $p47^{phox}$ or NOX1 effectively blocked K-Ras-induced ROS generation, anchorage-independent colony formation and tumor formation. Taken together, our findings demonstrated that oncogenic K-Ras activates the signaling cascade p38/PDPK1/PKCδ/$p47^{phox}$/NOX1 for ROS generation and consequent malignant cellular transformation.
Cell Death and Differentiation (2014) **21,** 1185–1197; doi:10.1038/cdd.2014.34; published online 14 March 2014

Many studies have suggested that reactive oxygen species (ROS) are not merely harmful by-products but also serve as signaling molecules involved in many cellular pathways such as growth factor signaling,[1,2] inflammatory response[3] and apoptosis.[4] Consistent with this view, intracellular ROS are generated purposely by plasma membrane-bound nicotinamide adenine dinucleotide phosphate (NADPH) oxidase complexes.[5] As ROS displays both beneficial as a signaling molecule and harmful effects as oxidative by-products, the pathways that regulate ROS homeostasis may be crucial in cellular function. Aberrantly increased intracellular ROS has been often implicated in a large number of diseases including atherosclerosis, pulmonary fibrosis, cancer, neurodegenerative diseases and aging.[6–8] In cancers, as highly reactive molecules, ROS act as mutagenic and may thereby promote cancers. Also, ROS promote cancer progression by participating in oncogenic signaling pathways such as Ras, c-Myc and c-Src.[9–11] Indeed, Ras-induced ROS generation caused to increase the activation of mitogen-activated protein kinase (MAPK) and DNA-binding activities of the transcription factors such as activator protein-1, activator protein-2 and nuclear factor-κB in rat kidney epithelial cells,[12] suggesting that ROS participate in cell signaling.

GTPases of the Ras family of oncogenes transduce extracellular signals to the nucleus, acting as molecular switches in signaling networks that connect a variety of upstream signals to a wide array of downstream signaling pathways. Ras mutations are found in around 30% of all human malignancies, with K-Ras being the most frequently activated oncogene in cancer cells.[13,14] Notably, aberrant activation of Ras alone was found to be sufficient to transform mammary epithelial cells into malignant cells. Although the underlying mechanisms remain obscure, several lines of evidence suggested the functional role of ROS in Ras-induced cellular transformation.[12,15–17] In the previous study, constitutive expression of the active form of v-Ha-Ras caused cellular transformation, accompanying with ROS generation; however, overexpression of antioxidant enzymes such as manganese-containing superoxide dismutase or copper- and zinc-containing superoxide dismutase effectively inhibited Ras-induced transformation,[12,16] indicating that Ras induces cellular transformation through ROS production. In line with these studies, in human lung adenocarcinoma cells, the activity of K-Ras was correlated positively with the levels of ROS.[18] In lung epithelial cells, oncogenic K-Ras expression promoted ROS generation through cyclooxygenase (COX)-2, causing DNA damages and malignant transformation.[19]

[1]Laboratory of Molecular Biochemistry, Department of Life Science, Research Institute for Natural Sciences, Hanyang University, Seoul 133-791, Korea; [2]Research Center, Dongnam Institute of Radiological and Medical Sciences, Busan, Korea; [3]Low Dose Radiation Research Center, National Radiation Emergency Medical Science, Korea Institute of Radiological and Medical Sciences, Seoul 139-706, Korea and [4]Division of Radiation Cancer Biology, Korea Institute of Radiological and Medical Sciences, Seoul 139-706, Korea

*Corresponding author: S-J Lee, Laboratory of Molecular Biochemistry, Department of Life Science, Research Institute for Natural Sciences, Hanyang University, 17 Haengdang-Dong, Seongdong-Ku, Seoul 133-791, Korea. Tel: +82 2 2220 2557; Fax: +82 2 2299 0762; E-mail: sj0420@hanyang.ac.kr

[5]These authors contributed equally to this work.

Abbreviations: PKC, protein kinase C; PDPK1, 3-phosphoinositide-dependent protein kinase-1; MAPK, mitogen-activated protein kinase; NADPH, nicotinamide adenine dinucleotide phosphate-oxidase; DN, dominant-negative mutant form; ROS, reactive oxygen species; GST, glutathione S-transferases; siRNA, small interfering RNA; WT, wild type

Received 02.9.13; revised 04.2.14; accepted 05.2.14; Edited by N Chandel; published online 14.3.14

Although mitochondrial ROS production was suggested to be important for Ras-driven malignant transformation,[20] Ras increased ROS through NADPH oxidase 1 (NOX1) that is a plasma membrane-bound enzyme, finally causing malignant transformation.[21] However, the precise molecular mechanisms underlying K-Ras-induced ROS generation remain largely unknown.

In the present study, we demonstrate that K-Ras-induced ROS generation in normal fibroblasts is mediated by NOX1/p47^{phox}. Also, we show that only p38 among all MAPKs is involved in K-Ras-induced ROS generation and consequent cellular transformation. Importantly, K-Ras-induced activation of p38 led to an activation of PDPK1, which then signals through PKCδ, p47^{phox} and NOX1. In addition, we provide an evidence that the same signaling pathway is also driven by endogenous oncogenic K-Ras in cancer cells. Collectively, our findings suggest that oncogenic K-Ras activates the signaling axis p38/PDPK1/PKCδ/p47^{phox}/NOX1 for ROS generation and consequent cellular transformation.

Results

ROS is crucial for K-Ras^{V12}-induced cellular transformation. We examined whether K-Ras generates ROS in normal fibroblasts. To this end, Rat2 fibroblasts were transduced with K-Ras^{V12} that is a constitutively active mutant form of the protein. Notably, K-Ras^{V12} caused to increase DCFDA fluorescence (Figure 1a), indicating that intracellular ROS was increased in a time-dependent manner in K-Ras^{V12}-transduced cells, whereas low ROS levels were maintained in cells mock-transduced with a control vector, MFG (Figure 1a; Supplementary Figures S1A and B). Concomitant with ROS generation, K-Ras^{V12}-transduced cells acquired an anchorage-independent colony-forming phenotype (Supplementary Figure S1C). However, ectopic expression of the potent antioxidant enzymes catalase or glutathione peroxidase blocked the K-Ras^{V12}-induced ROS generation (Figure 1b) and suppressed the formation of anchorage-independent colonies caused by K-Ras^{V12} (Figure 1c). To further elucidate whether ROS are associated with K-Ras^{V12}-induced tumorigenesis, we subcutaneously injected K-Ras^{V12}-transduced or non-transduced cells, with or without transfected catalase, into nude mice. K-Ras^{V12}-transduced cells efficiently formed tumors in nude mice compared with non-transduced cells. However, catalase expression effectively blocked K-Ras^{V12}-induced tumorigenesis in nude mice (Figure 1d). Collectively, these results suggest that ROS has a key role in K-Ras^{V12}-induced transformation.

NOX1 and p47^{phox} are required for K-Ras-induced ROS generation. As non-phagocytic NADPH oxidases have been reported to contribute ROS generation in Ras-transfected fibroblasts,[21] we treated cells with small interfering RNAs (siRNAs) against large catalytic subunits of NADPH oxidase (Nox1, Nox2, Nox3 and Nox4), and then transduced with K-Ras^{V12} (Supplementary Figure S2A). Importantly, K-Ras^{V12}-induced ROS generation and anchorage-independent colony formation were suppressed by downregulation of Nox1, but not other Nox family members (Figures 2a and b). Because K-Ras^{V12}-induced ROS generation could occur in mitochondria, we examined the possibility by treatment with rotenone, a mitochondrial ROS blocker. However, rotenone did not affect ROS generation (data not shown), indicating that mitochondrial mechanisms are not involved in K-Ras-induced ROS generation. As Nox1 activity is regulated by the cytosolic regulatory subunit p47^{phox} or its homolog NOXO1,[22,23] cells were treated with siRNAs targeting p47^{phox} or NOXO1 (Supplementary Figure S2B). Downregulation of p47^{phox} inhibited K-Ras^{V12}-induced ROS generation and anchorage-independent colony formation, whereas siRNAs targeting NOXO1 did not (Figures 2c and d), suggesting that p47^{phox} has a crucial role in K-Ras^{V12}-induced activation of Nox1. Phosphorylation of p47^{phox} and its translocation to the plasma membrane have been shown to be key events for NADPH oxidase activation.[24] We therefore investigated whether K-Ras^{V12} induces phosphorylation and membrane translocation of p47^{phox}. To this end, we immunoprecipitated all phosphorylated proteins on serine, threonine or tyrosine residues. Importantly, p47^{phox} was detected only in immunoprecipitated proteins that are phosphorylated on serine residues, indicating that K-Ras^{V12} promotes phosphorylation of p47^{phox} at serine (Figure 2e). Taken together, these results suggest that K-Ras^{V12}-induced ROS generation mainly occurs through a Nox1/p47^{phox} pathway.

K-Ras-dependent phosphorylation of p47^{phox} is mediated by PKCδ and contributes to p47^{phox} translocation to the plasma membrane and ROS generation. Because PKC isozymes are involved in Ras-induced cellular transformation,[25] we examined the kinase activity of PKC isozymes in K-Ras^{V12}-transduced cells. Importantly, K-Ras^{V12} selectively increased the kinase activity of PKCδ among the isozymes (Figure 3a). Also, when cells were transfected with dominant-negative (DN) mutant forms of PKC isozymes, only DN-PKCδ suppressed K-Ras^{V12}-induced ROS generation and anchorage-independent colony formation, whereas DN-PKCα and DN-PKCβ had no effect on these phenotypes (Figures 3b and c). In agreement, DN-PKCδ effectively suppressed K-Ras^{V12}-induced tumor formation in xenograft mice, (Figure 3d). These results suggest that PKCδ has a pivotal role in K-Ras^{V12}-induced ROS generation and cellular transformation.

As p47^{phox} was phosphorylated on the serine residue in a K-Ras^{V12}-dependent manner, we next assessed whether PKCδ catalyzes the phosphorylation of p47^{phox}. To examine this possibility, cells were transfected with each DN PKC isoform and then transduced with K-Ras^{V12}. Notably, when cells are transfected with DN-PKCδ, p47^{phox} was not detected in serine-phosphorylated proteins immunoprecipitated with an anti-phospho-serine antibody (Figure 3e). Also, DN-PKCδ attenuated K-Ras^{V12}-induced translocation of p47^{phox} to the membrane fraction, indicating that PKCδ is responsible for the activation and translocation of p47^{phox} to membrane-anchored NOX1. We next examined whether PKCδ interacts directly with p47^{phox} by GST-p47^{phox} pull-down assays. Notably, PKCδ was co-precipitated with GST-p47^{phox}-coupled glutathione-sepharose, indicating that PKCδ interacts with p47^{phox} (Figure 3f). To further examine the PKCδ-mediated

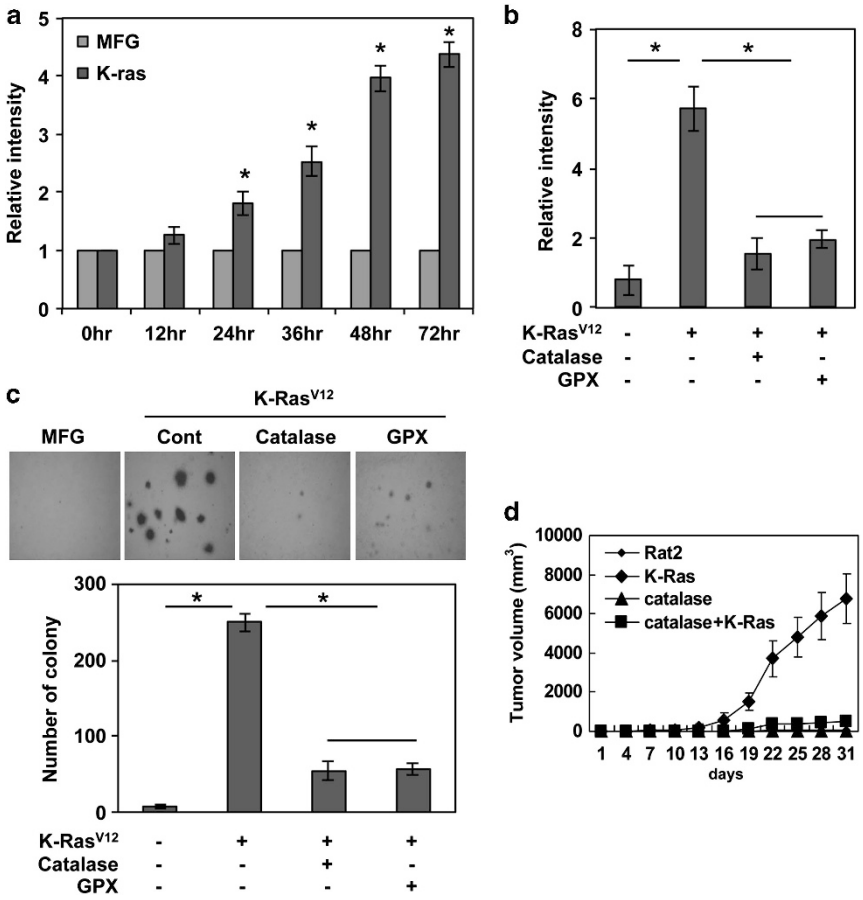

Figure 1 K-Ras^{V12} expression causes ROS generation and consequent malignant transformation in normal fibroblasts. (**a**) Levels of ROS as assessed by dichloro-dihydro-fluorescein diacetate (DCFDA). ROS is gradually increased in Rat2 fibroblasts after transduction with K-Ras^{V12}, compared with control vector MFG-transduced cells. (**b**) Levels of ROS as assessed by DCFDA fluorescence. Ectopic expression of antioxidant enzymes catalase or GPX blocks K-Ras-induced ROS generation. (**c**) Anchorage-independent colony formation in soft agar. Ectopic expression of antioxidant enzymes catalase or GPX attenuates K-Ras-induced colony-forming ability in soft agar. (**d**) Tumor formation in xenograft mice. Ectopic expression of antioxidant enzymes catalase or GPX in Rat2 fibroblasts suppresses K-Ras-induced tumor formation. Error bars represent mean ± S.D. of triplicate samples. *$P<0.001$

phosphorylation of p47^{phox}, we performed immune complex kinase assays using GST-p47^{phox} as a substrate. Importantly, PKCδ phosphorylated GST-p47^{phox}, whereas PKCα and PKCβ did not (Figure 3g). Collectively, these results suggest that PKCδ directly binds to and phosphorylates p47^{phox} in a K-Ras^{V12}-dependent manner.

PKCδ-induced phosphorylation of Ser348 and Ser379 residues in p47^{phox} is critical for oncogenic K-Ras-induced ROS generation and cellular transformation. To find out the domain of p47^{phox} that interacts with PKCδ, we cloned each domain of p47^{phox} that is phox homology (PX), N- and C-terminal SH3 (SH3-N, SH3-C) and polybasic/proline-rich (PP) domains, as well as the full length of p47^{phox} into pGEX-2T, and purified the GST-fusion proteins for GST pull-down assays. Notably, PKCδ was co-precipitated with GST-SH3-N as well as full-length GST-p47^{phox} in lysates of K-Ras^{V12}-transduced cells, but not with other domains (Figures 4a and b). To confirm this result, we cloned FLAG-tagged full-length p47^{phox} into pFLAG-CMV2 and the HA-tagged domain of p47^{phox} (PX, SH3-N, SH3-C and PP) into pCMV-HA. Consistently, PKCδ is co-immunoprecipitated with the SH3-N domain and full-length p47^{phox} (Figures 4a and c). These results suggest that PKCδ interacts with the SH3-N domain of p47^{phox} in a K-Ras^{V12}-dependent manner.

As PKCδ interacts directly with p47^{phox}, we next examined which serine residues of p47^{phox} are phosphorylated by PKCδ. To this end, we generated GST-fusion protein p47^{phox} harboring a point mutation (S345A, S348A, S359A, S370A, S379A, S348/379A and S345/359A) and compared them with wild type as substrates in PKCδ kinase assays. Though PKCδ phosphorylated the wild-type GST-p47^{phox} substrate in the kinase assay, it failed to phosphorylate p47^{phox} harboring point mutation S348A or/and S379A substitutions (Figure 4d), indicating that PKCδ phosphorylates Ser348 and Ser379 in p47^{phox}. To further confirm, we performed PKCδ kinase assays in a cell-free system using recombinant, active PKCδ. Consistently, recombinant PKCδ displayed reduced catalytic activity toward the GST-S348A, GST-S379A and GST-S348/379A point-mutant forms of p47^{phox} compared with other mutants (Supplementary Figure S3). These results suggest that PKCδ phosphorylates Ser348 and Ser379 of p47^{phox} in a K-Ras^{V12}-dependent manner.

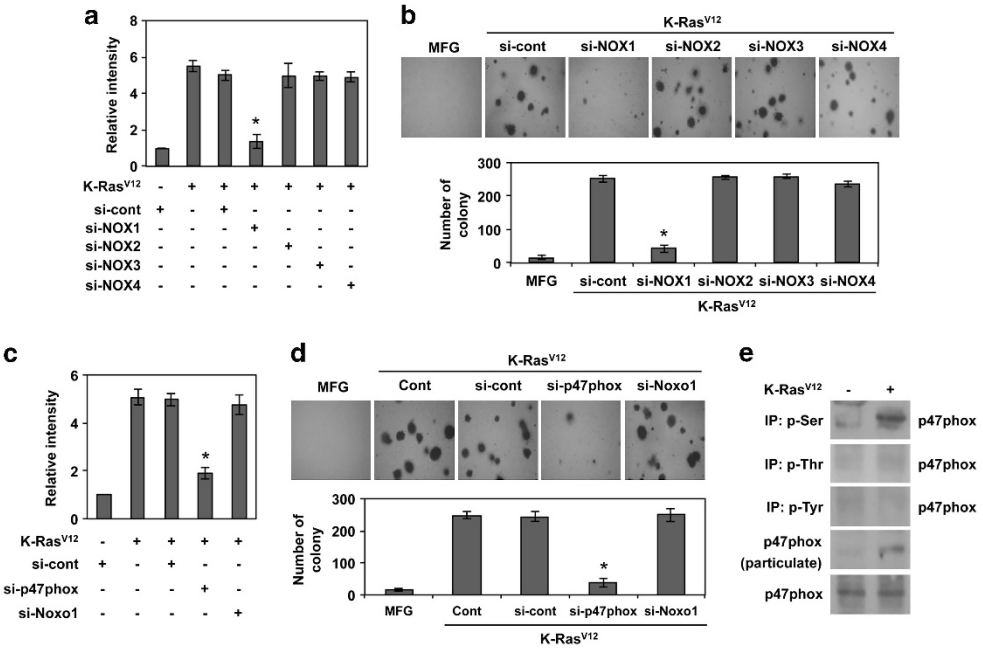

Figure 2 NOX1 and p47^{phox} are required for K-Ras-induced ROS generation and subsequent malignant transformation. (**a**) Levels of ROS as assessed by DCFDA fluorescence in Rat2 cells or K-Ras^{V12}-transduced cells after transfection with siRNA targeting NOX1, NOX2, NOX3, NOX4, or scrambled siRNA. (**b**) Soft agar colony formation of K-Ras-transduced cells after transfection with siRNA targeting NOX1, NOX2, NOX3, NOX4, or scrambled siRNA and control vector MFG-transduced cells. (**c**) Levels of ROS as assessed by DCFDA fluorescence in K-Ras^{V12}-transduced cells after transfection with siRNA targeting p47^{phox}, Noxo1, or scrambled siRNA. (**d**) Soft agar colony formation of K-Ras^{V12}-transduced cells after transfection with siRNA targeting p47^{phox}, Noxo1, or scrambled siRNA and control vector MFG-transduced cells. (**e**) Western blot analysis for p47^{phox} after immunoprecipitation with anti-phospho-serine, -phospho-threonine or -phospho-tyrosine antibody or particulate after separation of cytosol and particulate. Error bars represent mean ± S.D. of triplicate samples. *$P < 0.001$

We next examined whether Ser348 and/or Ser379 residues of p47^{phox} are critical for the interaction with PKCδ and translocation of p47^{phox} to the plasma membrane. To this end, we cloned the HA-tagged p47^{phox} mutant forms HA-S345A, HA-S348A, HA-S359A, HA-S370A, HA-S379A, HA-S348/379A and HA-S345/359A, as well as wild-type HA-tagged p47^{phox}. After cells were transfected with these constructs and then transduced with K-Ras^{V12}, HA-tagged p47^{phox} was immunoprecipitated with an anti-HA antibody. Notably, PKCδ was co-immunoprecipitated with all point-mutant forms of p47^{phox}, indicating that Ser348 and/or Ser379 residues are not critical for the interaction with PKCδ (Figure 4e). Notably, however, HA-S348A, HA-S379A and HA-S348/379A point-mutant forms were not detected in the membrane fraction, whereas other mutant forms were. These results suggest that phosphorylation of p47^{phox} at Ser348 and Ser379 is crucial for its membrane translocation and activation of NOX1. In agreement, transfection with S348A, S379A or S348/379A mutant forms of p47^{phox} attenuated the K-Ras^{V12}-induced ROS and anchorage-independent colony-forming ability (Figures 4f and g). Collectively, these results suggest that PKCδ-mediated phosphorylation of p47^{phox} at Ser348 and Ser379 is crucial for K-Ras^{V12}-induced ROS generation and cellular transformation.

K-Ras-induced activation of p38 is required for ROS generation and cellular transformation. As oncogenic Ras is known to activate multiple downstream signaling including MAPK family members,[26,27] we examined whether K-Ras^{V12} activates ERK, p38 and JNK. As expected, K-Ras^{V12} expression resulted in activation of all three MAPKs (Figure 5a). Importantly, transfection with DN-p38 effectively suppressed K-Ras^{V12}-induced ROS generation, whereas DN-ERK or DN-JNK had no such effect (Figure 5b). Consistently, treatment with the specific p38 inhibitor SB203580 decreased K-Ras^{V12}-induced ROS (Figure 5c), indicating that p38 is a downstream effector of K-Ras^{V12} for ROS generation. In agreement, transfection with DN-p38 attenuated K-Ras^{V12}-induced anchorage-independent colony formation (Figure 5d). Intriguingly, despite the fact that ERK was not involved in ROS generation, DN-ERK suppressed K-Ras^{V12}-induced colony formation, suggesting that ERK participates in K-Ras^{V12}-induced cellular transformation in a ROS-independent manner. To further confirm that p38 is a downstream effector of K-Ras^{V12}-induced cellular transformation, we subcutaneously inoculated cells that express both DN-p38 and K-Ras^{V12} into athymic nude mice, and monitored tumor formation. Notably, DN-p38 effectively attenuated K-Ras^{V12}-induced tumorigenesis in mice (Figure 5e). Collectively, these results suggest that p38 has a pivotal role in K-Ras^{V12}-induced ROS generation and consequent cellular transformation.

To further elucidate the role of p38 in K-Ras^{V12}-induced malignant transformation, we examined whether p38 acts as an upstream signal of PKCδ. To this end, we determined the amino acid of PKCδ that is phosphorylated in a K-Ras^{V12}-dependent manner. By immunoprecipitation using antibodies against phospho-serine, phospho-threonine or phospho-tyrosine residues, we found that PKCδ is phosphorylated on Tyr and Thr residues in a K-Ras^{V12}-dependent manner (Supplementary Figure S4A). In a further analysis, the kinase

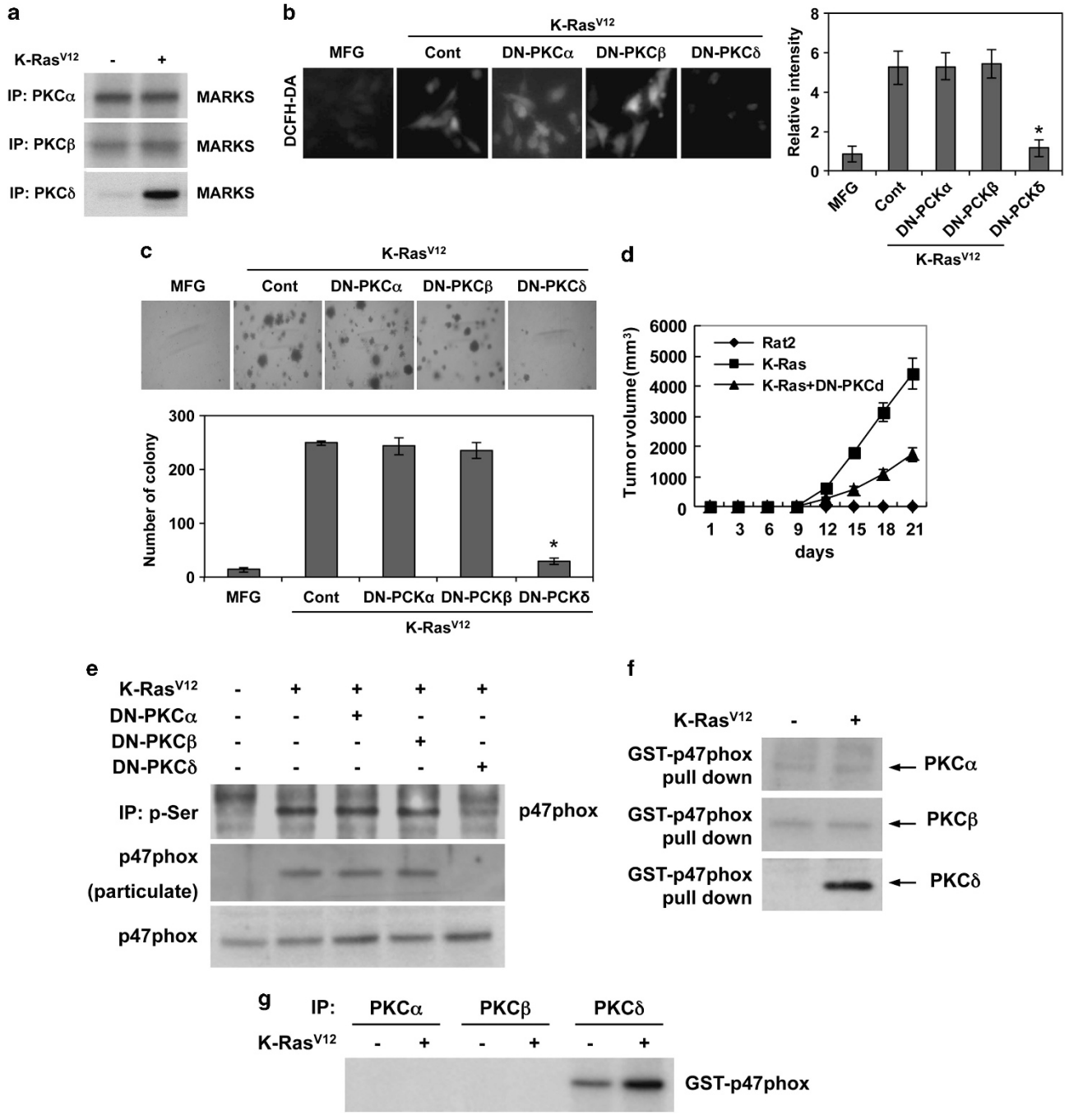

Figure 3 PKCδ phosphorylates p47^{phox} for K-Ras-induced ROS generation. (**a**) Kinase assay for PKC-α, -β, -δ in K-Ras^{V12}-transduced cells and control vector MFG-transduced cells with MARKS as substrate. (**b**) Levels of ROS as assessed by DCFDA fluorescence in control vector MFG-transduced cells or cells transfected with DN-PKCα, DN-PKCβ, DN-PKCδ, or control pcDNA and subsequently transduced with K-Ras^{V12}. (**c**) Soft agar colony formation in control vector MFG-transduced cells or cells transfected with dominant-negative mutant PKCα, PKCβ, PKCδ, or control vector pcDNA and subsequently transduced with K-Ras^{V12}. (**d**) Tumor growth curves of xenografts derived from parental Rat2 cells, K-Ras^{V12}-transduced cells, or K-Ras^{V12}-transduced cells that are transfected with DN-PKCδ. (**e**) Western blot for p47^{phox} after immunoprecipitation with anti-phospho-serine antibody in control vector MFG-transduced cells or cells that are transfected with DN-PKCδ and subsequently are transduced with K-Ras^{V12}. Also, western blot for p47^{phox} in particulate after separation of cytosol and particulate in cell lysates. (**f**) Western blot for PKC-α, -β, -δ after GST pull-down of p47^{phox} in K-Ras^{V12}-transduced cells and control vector MFG-transduced cells. (**g**) Kinase assay of PKCα, PKCβ, and PKCδ with GST-p47^{phox} fusion protein as substrate in K-Ras^{V12}-transduced and control vector MFG-transduced cells. Error bars represent mean ± S.D. of triplicate samples. *$P<0.001$

assay of PKCδ with a point mutation on Tyr311, Thr505, Tyr523 or Tyr565 revealed that phosphorylation on Thr505 is necessary for PKCδ kinase activity toward p47^{phox} (Supplementary Figure S4B). In agreement, K-Ras^{V12} increased phosphorylation of PKCδ at Thr505 (Supplementary Figure S4C). Supporting these results, several evidences suggested that the phosphorylation of PKCδ on Thr505 is associated with kinase activity.[28,29]

Thus, we analyzed the phosphorylation status of PKCδ on Thr505 after transfection with DN-p38. Notably, K-Ras^{V12}-induced phosphorylation of Thr505 in PKCδ was blocked by DN-p38 (Figure 5f). In line with this, DN-p38 displayed same effects that we observed when PKCδ was inhibited, indicating that K-Ras^{V12} activates PKCδ through p38 MAPK. DN-p38, but not DN-ERK or DN-JNK, decreased the interaction between p47^{phox} and PKCδ (Figure 5g). Also, DN-p38 inhibited K-Ras^{V12}-induced phosphorylation at serine residues of p47^{phox} (Figure 5h). In agreement, transfection with wild-type p38 increased the interaction of p47^{phox} with PKCδ, p47^{phox} phosphorylation and translocation to the plasma membrane;

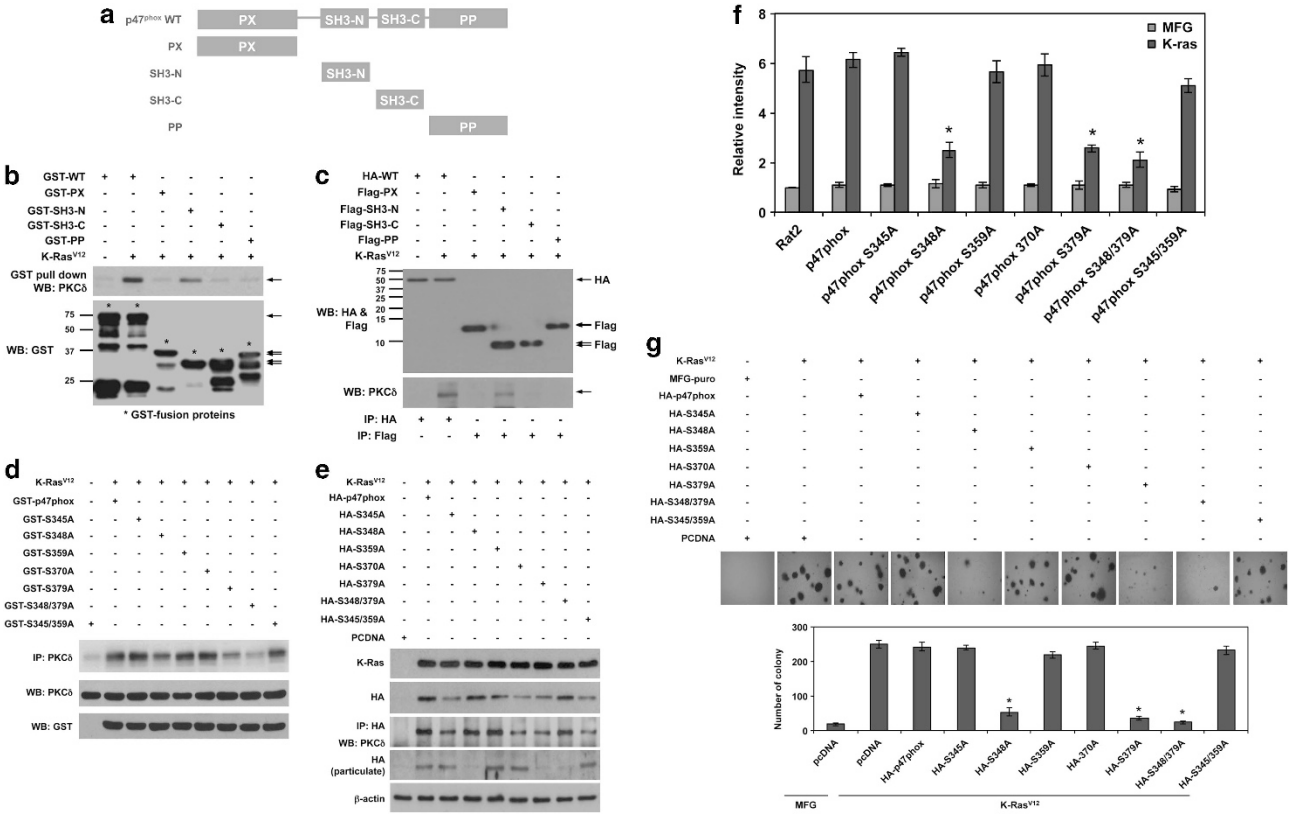

Figure 4 PKCδ binds to the SH3-N domain and phosphorylates Ser348 and Ser379 residues in p47^{phox} for K-Ras^{V12}-induced ROS generation and consequent malignant transformation. (**a**) Constructs of GST-fusion proteins for the full length, PX domain, SH3-N domain, SH3-C domain, and PP domain in p47^{phox}. (**b**) Western blot for PKCδ and GST after GST pull-down of GST-fusion proteins in cells that are transfected with each construct of the GST-fusion protein and are subsequently transduced with K-Ras^{V12}. (**c**) Western blot for HA and Flag in cells that are transfected with HA-tagged WT p47^{phox} or Flag-tagged-PX, -SH3-N, -SH3-C, -PP domains in cells that are transfected with each construct of the GST-fusion protein and are subsequently transduced with K-Ras^{V12}. Also, western blot for PKCδ after immunoprecipitation with anti-HA or -Flag antibody in cells that are transfected with each construct of the GST-fusion protein and are subsequently transduced with K-Ras^{V12}. (**d**) Kinase assay of PKCδ with GST-fusion protein p47^{phox} wild type or mutant form, as substrate, that harbors a point mutation on Ser345, -348, -359, -370, -379 to Ala. (**e**) Western blot for PKCδ after immunoprecipitation with anti-HA antibody in cells that are transfected with HA-tagged WT p47^{phox} or HA-tagged p47^{phox} that harbors a point mutation on Ser345, -348, -359, -370, -379, -348/379, -345/359 to Ala. Also, western blot for HA to detect HA-tagged WT p47^{phox} or HA-tagged p47^{phox} that harbors a point mutation on Ser345, -348, -359, -370, -379, -348/379, -345/359 to Ala, in particulate after separation of cytosol and particulate in cell lysates. (**f**) Levels of ROS as assessed by DCFDA fluorescence in cells that are transfected with WT p47^{phox} or mutant p47^{phox} harboring a point mutation on Ser345, -348, -359, -370, -379, -348/379, -345/359 to Ala, and are subsequently transduced with K-Ras^{V12} or control vector MFG. (**g**) Soft agar colony formation in control cells or cells that are transfected with WT p47^{phox} or mutant p47^{phox} harboring a point mutation on Ser345, -348, -359, -370, -379, -348/379, -345/359 to Ala, and are subsequently transduced with K-Ras^{V12}. WT, wild type; Error bars represent mean ± S.D. of triplicate samples. *$P<0.001$

Figure 5 K-Ras^{V12}-induced activation of p38 is required for ROS generation and consequent malignant transformation. (**a**) Western blot for activation status of ERK, p38, and JNK MAPK in K-Ras^{V12}-transduced cells and control vector MFG-transduced cells. (**b** and **c**) Levels of ROS as assessed by DCFDA fluorescence in cells that are transfected with DN-ERK, DN-p38, or DN-JNK (**b**) or treatment with SB203580, inhibitor specific to p38 MAPK (**c**), and are subsequently transduced with K-Ras^{V12}. (**d**) Soft agar colony formation in control cells or cells that are transfected with DN-ERK, DN-p38, or DN-JNK, and are subsequently transduced with K-Ras^{V12}. (**e**) Tumor growth curves of xenografts derived from parental Rat2 cells, K-Ras^{V12}-transduced cells, or K-Ras^{V12}-transduced cells that are transfected with DN-p38. (**f**) Western blot for the phosphorylation status on Thr505 of PKCδ in Rat2 cells that are transfected with DN-p38 or control pcDNA, and are subsequently transduced with K-Ras^{V12} or control vector MFG. (**g**) Western blot for the analysis of interaction between PKCδ and p47^{phox} after GST-p47^{phox} pull-down and immunoprecipitation with anti-PKCδ in cells that are transfected with DN-ERK, DN-p38, or DN-JNK, and are subsequently transduced with K-Ras^{V12}. (**h**) Western blot for phosphorylation status on serine residues of p47^{phox} after immunoprecipitation with anti-phospho-serine antibody, or membrane translocation of p47^{phox} in cells that are transfected with DN ERK, DN-p38, or DN-JNK, and are subsequently transduced with K-Ras^{V12}. (**i**) Western blot for the analysis of interaction between PKCδ and p47^{phox} after co-immunoprecipitation with anti-p47^{phox} or anti-PKCδ antibody in cells that are transfected with WT p38 or control pcDNA, and are subsequently transduced with K-Ras^{V12} or control vector MFG. (**j**) Levels of ROS as assessed by DCFDA fluorescence in cells that are transfected with WT p38 or control pcDNA, and are subsequently transduced with K-Ras^{V12} or control vector MFG. WT, wild type; DN, dominant-negative mutant; Error bars represent mean ± S.D. of triplicate samples. *$P<0.001$

these effects were also observed in the presence of K-Ras^{V12}, albeit to a lesser extent (Figure 5i). Overexpression of p38 also increased ROS generation, an effect that was greater in the absence than presence of K-Ras^{V12} (Figure 5j). Collectively, these results suggest that K-Ras^{V12} activates the p38/PKCδ/p47^{phox}/NOX1 signaling axis for ROS generation.

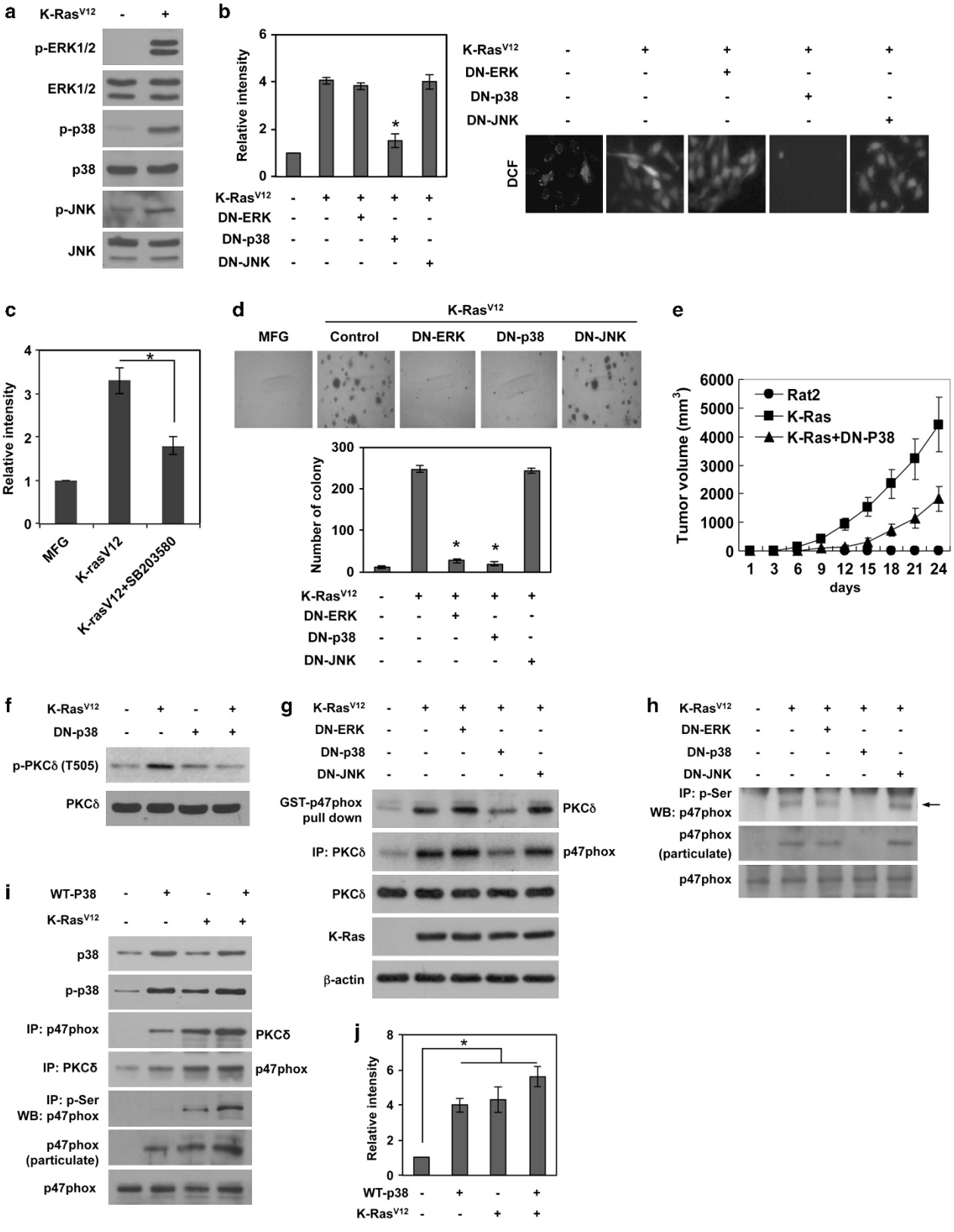

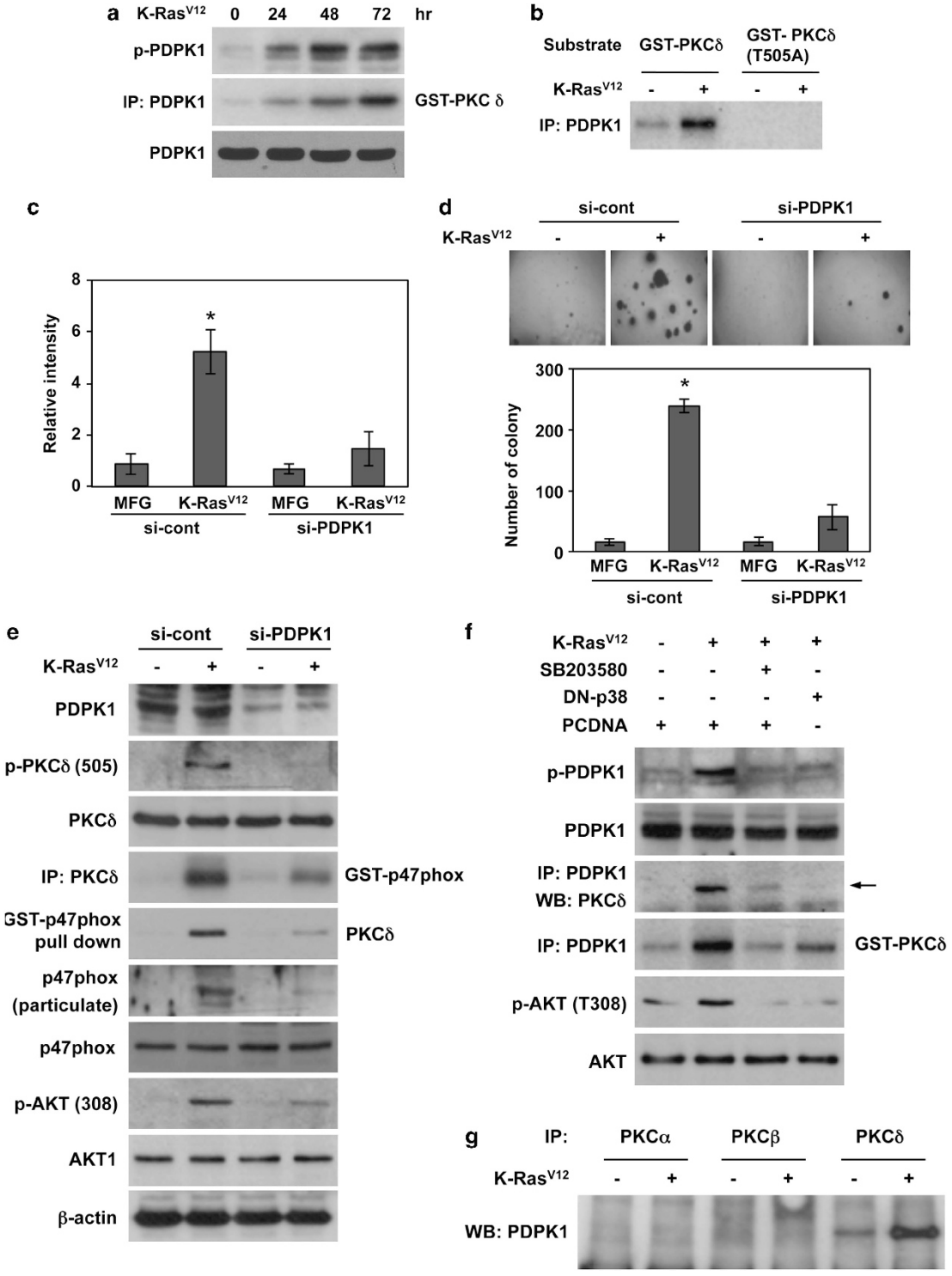

Figure 6 PDPK1 interacts with and phosphorylates PKCδ for K-Ras-induced ROS generation and consequent malignant transformation. (**a**) Western blot analysis for phosphorylation status and kinase assay of PDPK1 using GST-PKCδ as substrate at 0, 24, 48, 72 h after transduction with K-Ras^{V12}. (**b**) Kinase assay of PDPK1 using GST-PKCδ or GST-PKCδ (T505A) as substrate in cells that are transduced with K-Ras^{V12} or control vector MFG. (**c**) Levels of ROS as assessed by DCFDA fluorescence in cells that are transfected with siRNA targeting PDPK1 or control scrambled siRNA, and are subsequently transduced with K-Ras^{V12} or control vector MFG. (**d**) Soft agar colony formation in cells that are transfected with siRNA targeting PDPK1 or control scrambled siRNA, and are subsequently transduced with K-Ras^{V12} or control vector MFG. (**e**) Western blot analysis for phosphorylation status and kinase assay of PKCδ using GST-p47^{phox} as substrate, and membrane translocation of p47^{phox} in cells that are transfected with siRNA targeting PDPK1 or control scrambled siRNA, and are subsequently transduced with K-Ras^{V12} or control vector MFG. (**f**) Western blot analysis for phosphorylation status, interaction with PKCδ and kinase assay using GST-PKCδ as substrate, of PDPK1. (**g**) Western blot for PDPK1 after immunoprecipitation with anti-PKC-α, -β, -δ antibody as indicated in cells that are transduced with K-Ras^{V12} or control vector MFG. Error bars represent mean ± S.D. of triplicate samples. *$P<0.001$

p38-mediated activation of PDPK1 is necessary for K-Ras^{V12}-induced PKCδ/p47^{phox} signaling and subsequent ROS generation and cellular transformation. PDPK1 was first identified based on its ability to phosphorylate Thr308 of AKT.[30–32] However, conservation of amino-acid sequences similar to those surrounding Thr308 of AKT in the AGC family of Ser/Thr protein kinases suggested that PDPK1 may phosphorylate other AGC protein kinase family members, including PKC isoforms. In agreement with this, recent reports have demonstrated that PDPK1 can phosphorylate PKC isoforms.[33] Thus, we examined whether PDPK1 activates PKCδ, thereby participating in K-Ras^{V12}-induced ROS generation. To this end, we examined whether PDPK1 is activated by K-Ras^{V12}. Importantly, the phosphorylation of PDPK1 was increased with expression of K-Ras^{V12}, indicating that the activity of PDPK1 depends on K-Ras^{V12} (Figure 6a). Thus, we examined whether PDPK1 can phosphorylate PKCδ in a K-Ras^{V12}-dependent manner. Importantly, kinase assays showed that PDPK1 phosphorylates wild-type PKCδ but not the T505A mutant form (Figure 6b). In agreement with these results, the T505A mutant form of PKCδ showed a marked loss in affinity for p47^{phox} in the GST pull-down assay (Supplementary Figure S4B). In parallel, treatment with siRNA targeting PDPK1 inhibited K-Ras^{V12}-induced ROS generation and anchorage-independent colony formation (Figures 6c and d). Furthermore, downregulation of PDPK1 suppressed PKCδ phosphorylation and interaction with p47^{phox}, and decreased p47^{phox} translocation to the plasma membrane (Figure 6e). These results indicate that PDPK1 participates directly in the K-Ras^{V12}-induced signaling axis for ROS generation.

As p38 activated PKCδ in K-Ras^{V12}-transduced cells, we tested whether p38 activates PKCδ through PDPK1. To this end, we inhibited p38 activity by treatment with the specific p38 inhibitor, SB2003580, or transfection with DN-p38. Importantly, inhibition of p38 attenuated K-Ras^{V12}-induced phosphorylation of PDPK1 and reduced its kinase activity toward PKCδ (Figure 6f). In addition, immunoprecipitation showed that PDPK1 interacts with PKCδ in a K-Ras^{V12}-dependent manner, an interaction that was abolished by inhibition of p38 (Figures 6f and g). In contrast, treatment with the specific JNK inhibitor, SP600125 or ERK inhibitor PD98059, had no such effects (Supplementary Figure S4D). Taken together, these results suggest that K-Ras^{V12} induces ROS generation and subsequent cellular transformation through activation of the p38/PDPK1/PKCδ/p47^{phox}/NOX1 signaling axis.

Endogenous oncogenic K-Ras promotes ROS generation in cancer cells, driving the same signaling pathway as an exogenous K-Ras^{V12} in normal fibroblasts. In the above data, when exogenous K-Ras^{V12} is introduced into normal fibroblasts, we observed that K-Ras^{V12} induces ROS generation by triggering the signaling cascade, p38/PDPK1/PKCδ/p47^{phox}/NOX1, consequently causing cellular transformation. We next examined whether the K-Ras-driven signaling cascade for ROS generation is also valid in cancer cells that have an oncogenic K-Ras mutation. To examine the possibility, we chose HCT116 and SW480 colon cancers that harbor the oncogenic mutant form of K-Ras. Of importance, likely to the effect of K-Ras^{V12} in normal fibroblasts, siRNA-mediated downregulation of K-Ras caused to decrease the intracellular ROS in both cancer cell lines (Figure 7a), indicating that endogenous oncogenic K-Ras contributes to ROS generation. We next examined whether the oncogenic K-Ras promotes ROS generation in cancer cells through the signaling cascade p38/PDPK1/PKCδ/p47^{phox}/NOX1 as in normal fibroblasts. Notably, downregulation of K-Ras inhibited the signaling components such as p38, PDPK1 and PKCδ (Figure 7b). In line with these results, treatment with an inhibitor specific to p38 decreased ROS generation in both cancer cells (Figure 7c). Also, treatment with siRNA targeting either PDPK1 or p47^{phox} decreased the intracellular ROS in both cancer cell lines (Figure 7d; Supplementary Figure S4E). Taken together, these results suggest that aberrant activation of K-Ras increases intracellular ROS in both cancer and normal fibroblasts through the signaling cascade, p38/PDPK1/PKCδ/p47^{phox}/NOX1.

Discussion

Many studies have suggested that K-Ras-induced ROS generation is responsible for cellular transformation.[11,20,21] In line with these studies, we observed that K-Ras^{V12} transforms normal fibroblasts in association with ROS generation, causing acquisition of anchorage-independent colony-forming ability and increased tumor-forming capacity. In this study, we found that K-Ras^{V12}-induced ROS generation occurs through NOX1. For full activation, NOX1 requires the cytosolic regulatory subunit NOXO1 (NOX organizing protein-1) or, alternatively, the NOXO1 homolog p47^{phox}. Importantly, we found that K-Ras^{V12} promotes the activation of NOX1 through p47^{phox}. In addition, PKCδ among PKC isozymes was selectively activated in a K-Ras-dependent manner. Notably, PKCδ directly interacted with the tandem SH3-N domain of p47^{phox} and phosphorylated Ser348, -379 residues, promoting p47^{phox} translocation to the membrane fraction. The inactive form of p47^{phox} tends to adopt a closed form in which its two SH3 domains are masked through an intramolecular interaction with a polybasic/autoinhibitory region in the C terminus.[34] Activation and translocation of p47^{phox} to the membrane fraction requires phosphorylation of p47^{phox} at serine residues in the polybasic region/autoinhibitory region and PP domain, which induces a conformational change that leads to the exposure of two SH3 domains.[23] The exposed SH3 domains of p47^{phox} can directly interact with p22^{phox},[23] allowing membrane translocation of p47^{phox} and activation of NADPH oxidase. In this study, we found that PKCδ directly binds to the SH3-N domain of p47^{phox} in K-Ras^{V12}-expressing cells (Figure 4). It is likely that the direct binding of PKCδ to the SH3-N domain in p47^{phox} increases the proximity and orientation of the active site in PKCδ, facilitating its phosphorylation on Ser348, -379 in p47^{phox}. In agreement, DN-PKCδ inhibited translocation of p47^{phox} to the plasma membrane and blocked K-Ras-induced ROS generation, anchorage-independent colony formation and tumor formation. Previously, PKCδ has been reported to be implicated in the activation of NADPH oxidase in many cell lines.[35–37] However, the molecular mechanisms by which PKCδ

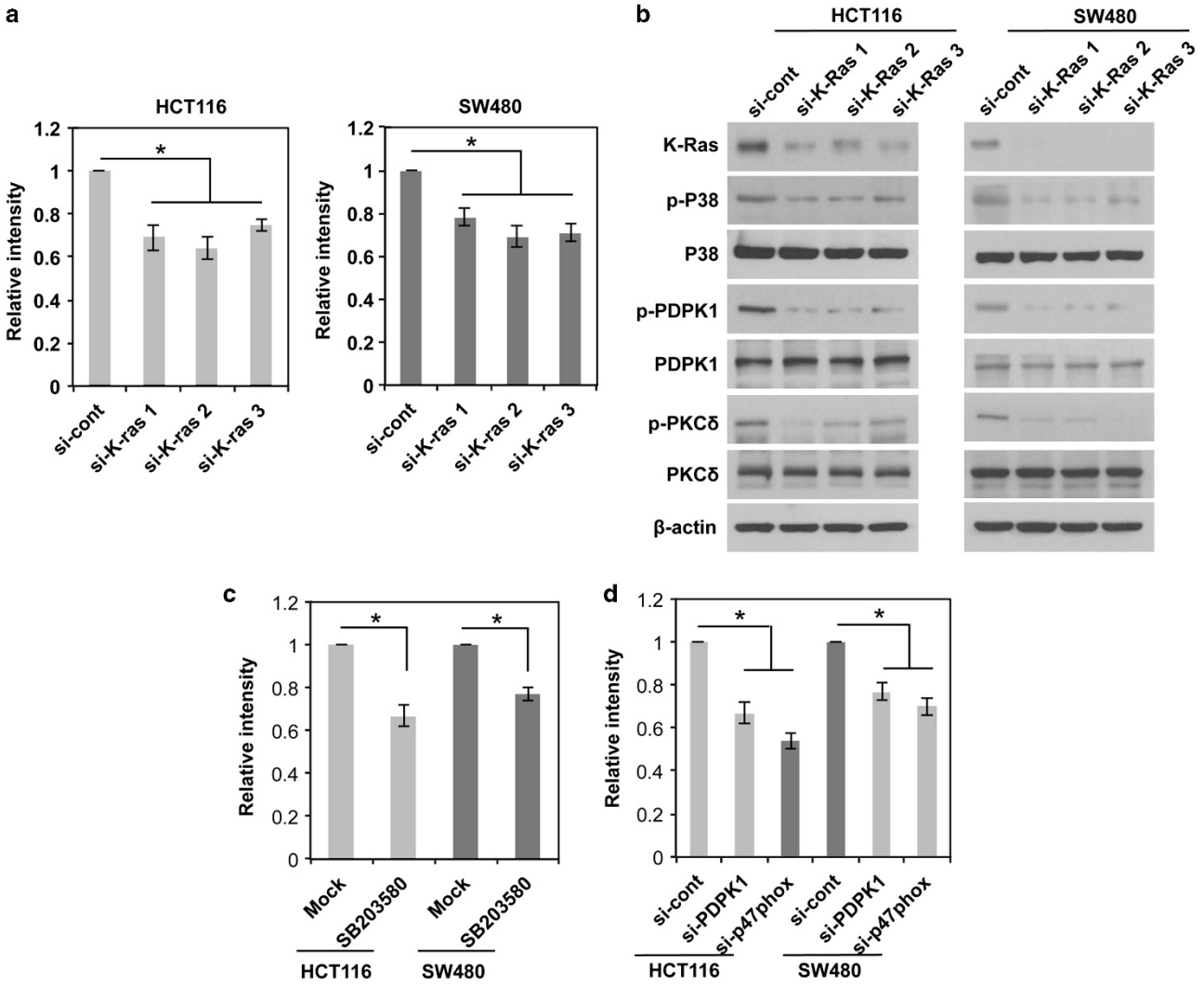

Figure 7 K-Ras-induced ROS generation in human cancer cell lines, driving the same signaling pathway as in normal fibroblasts. (**a**) Levels of ROS as assessed by DCFDA fluorescence in HCT116 and SW480 after transfection with three different siRNA-targeting K-Ras. (**b**) Western blot for activation status of p38, PDPK1, and PKCδ after transfection with three different siRNA-targeting K-Ras. (**c** and **d**) Levels of ROS as assessed by DCFDA fluorescence after treatment with SB203580, inhibitor specific to p38 MAPK (**c**) or siRNA targeting PDPK1 or p47^{phox} (**d**) in HCT116 and SW480. Error bars represent mean $\pm$ S.D. of triplicate samples. *$P<0.001$

activates NADPH oxidase have not been elucidated. In this study, we report that PKCδ directly binds to p47^{phox} and phosphorylates Ser348, -379, promoting its translocation to the membrane fraction and activation of NOX1.

PDPK1, known to have a key role in linking phosphoinositol 3-kinase (PI3K) to AKT, has been reported to be aberrantly overexpressed in breast cancers.[38,39] Furthermore, it was recently suggested that PDPK1 activation is a critical contributor to carcinogenesis and tumor maintenance in oncogenic K-Ras-driven pancreatic cancer.[40] Consistent with these studies, we found that PDPK1 is activated in K-Ras^{V12}-expressing cells and contributes to oncogenic K-Ras-induced ROS generation and cellular transformation (Figure 6). Conservation of amino-acid sequences similar to those surrounding Thr308 of AKT in the AGC family of Ser/Thr protein kinases suggests that PDPK1 might phosphorylate other protein kinases of the AGC family, including PKC isoforms. In agreement with this, recent reports have demonstrated that PDPK1 can phosphorylate PKC isoforms.[33] In this study, we found that PDPK1 binds and phosphorylates PKCδ at Thr505 in a K-Ras-dependent manner (Figure 6). In addition, down-regulation of PDPK1 attenuated a K-Ras-induced interaction between PKCδ and p47^{phox} and membrane translocation of p47^{phox} (Figure 6). As PKCδ interacts with PDPK1 as well as p47^{phox}, we suggest that PKCδ, PDPK1 and p47^{phox} proteins may form a signal transduction complex that facilitates K-Ras-induced ROS generation as shown in the schematic model (Figure 8).

Numerous studies have clearly shown that Ras induces activation of ERK, JNK and p38 MAPK signaling.[27,41,42] In line with these previous studies, we found that p38 is involved in K-Ras-induced ROS generation and malignant transformation. Inhibition of p38 blocked K-Ras-induced ROS generation, anchorage-independent colony formation and tumor formation. In parallel, overexpression of p38 increased ROS generation even in the absence of K-Ras^{V12}. Although

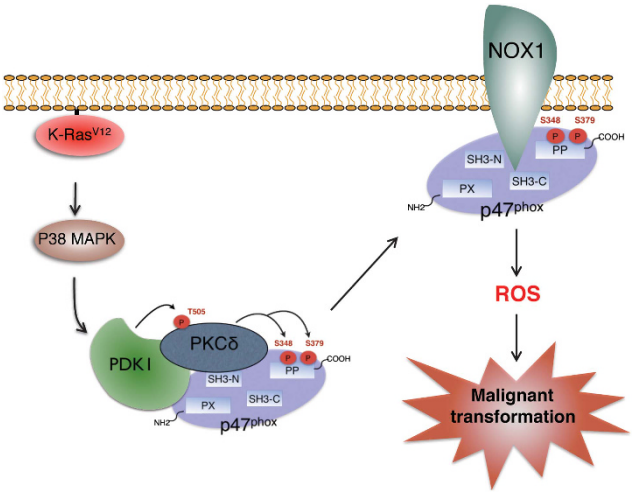

Figure 8 Schematic model for K-Ras-induced signaling cascade that leads to ROS generation and consequent malignant cellular transformation. Note that PKCδ, PDPK1, and p47^{phox} form a protein complex, thereby facilitating the signal cascade for ROS generation

inhibition of ERK blocked anchorage-independent colony formation, it did not affect ROS generation in K-Ras^{V12}-expressing cells, indicating that ERK might be involved in a ROS-independent pathway for K-Ras-induced malignant transformation. Extending our observation, we also found that, similarly to exogenous mutant K-Ras^{V12} in normal fibroblasts, endogenous oncogenic K-Ras in cancer cells induces ROS generation through the same signaling cascade.

Collectively, our data indicate that K-Ras^{V12} induces ROS generation via the signaling axis p38/PDPK1/PKCδ/p47^{phox}/NOX1 in cancer cells as well as normal fibroblasts. In agreement with this conclusion, inhibition of either component in this signaling axis effectively abolished K-Ras^{V12}-induced ROS generation and cellular transformation. Our findings may provide new insight into the molecular mechanisms governing K-Ras^{V12}-induced cellular transformation and cancer progression.

Materials and Methods

Chemical reagents and antibodies. Monoclonal anti-K-Ras antibody was purchased from Oncogene Science (Cambridge, MA, USA). Polyclonal antibodies against PKCα, PKCβ, PKCδ, phospho-JNK, JNK, p38 MAPK and monoclonal antibodies against phospho-ERK1/2 and ERK were purchased from Santa Cruz (Santa Cruz, CA, USA). Polyclonal anti-β-actin antibody and monoclonal antibodies against Flag-Tag and GST were purchased from Sigma-Aldrich Co (St. Louis, MO, USA). Monoclonal antibodies against p47^{phox} and phospho-tyrosine were purchased from Upstate Biotechnology Inc. (Lake Placid, NY, USA). Polyclonal antibodies against phospho-p38 MAPK, phospho-PDPK1 (Ser 241), PDPK1, phospho-PKCδ (Thr505), phospho-AKT (Thr 308), phospho-AKT (Ser 473), AKT1 and monoclonal antibodies against HA-Tag and ATF2 were purchased from Cell Signaling Technology (Beverly, MA, USA). Inhibitors specific to p38 MAPK (SB203580), PI3K/AKT (LY294002), JNK (SP600125) and MEK/ERK (PD98059), and recombinant active PKCδ, and monoclonal antibodies against phospho-serine and phospho-threonine were purchased from Calbiochem (San Diego, CA, USA). A monoclonal antibody against Rac1 was purchased from the BD Transduction Lab (San Jose, CA, USA).

Cell culture and siRNA transfection. Rat2 fibroblast cells were obtained from the American Type Culture Collection (Manassas, VA, USA) and were grown in RPMI 1640 medium (Gibco Invitrogen Corp, Paisley, UK) supplemented with 5% fetal bovine serum (FBS; Gibco Invitrogen Corp) and antibiotics at 37 °C in a humidified incubator with 5% CO_2. All oligonucleotides and siRNAs were purchased from Ambion Inc. (Austin, TX, USA). siRNA duplexes were introduced into cells using Lipofectamine 2000 reagent (Gibco Invitrogen Corp).

Production of a retroviral vector containing the oncogenic K-Ras gene. To generate MFG-K-RasV12, PCR fragments produced against pSPORT-K-RasV12 as templates were cloned into the MFG retroviral vector derived from murine Moloney leukemia virus. For retrovirus production, a modified 293T cell line was cultured in DMEM (Gibco Invitrogen Corp) supplemented with 10% FBS, 2 mmol/l GlutaMAX (Gibco Invitrogen Corp), 50 units/ml penicillin/streptomycin, 1 μg/ml tetracyclin, 2 μg/ml puromycin and 0.6 mg/ml G418 sulfate (Calbiochem) and transfected with MFG-K-RasV12 using the Lipofectamine 2000 reagent (Gibco Invitrogen Corp). At 48 h after the transfection, virus supernatant was harvested every day by replenishing with fresh medium for 5 days and passed through a 0.45-μm filter, and the viral supernatant was frozen at -80 °C. The supernatant was used for infection after adding 4 μg/ml Polybrene (Sigma-Aldrich Co).

Western blot analysis. It was performed as described earlier.[43] Briefly, cell lysates were prepared by extracting proteins with lysis buffer (40 mM Tris-HCl (pH 8.0), 120 mM NaCl, 0.1% Nonidet-P40) supplemented with protease inhibitors. Proteins were separated by SDS-PAGE and transferred to a nitrocellulose membrane. The membrane was blocked with 5% nonfat dry milk in Tris-buffered saline and incubated with primary antibodies for 1 h at room temperature. Blots were developed with peroxidase-conjugated secondary antibody, and proteins visualized by enhanced chemiluminescence (ECL; Amersham, Arlington Heights, IL, USA), following the manufacturer's recommendations.

Immunoprecipitation. Solubilized extracts (100–500 μg) in lysis buffer were precleared with protein A-Sepharose (Sigma-Aldrich Co), and the resulting supernatant fractions were incubated with a primary antibody (2 μg/ml) at 4 °C for 4 h. Immunoprecipitates were collected by incubating with protein A-Sepharose for 1 h, followed by centrifugation for 2 min at 4 °C. Pellets were washed five times with lysis buffer. Immunoprecipitates dissolved in SDS sample buffer were analyzed by western blotting, as described above.

Immune complex kinase assay. Proteins from 300 μg of cell extracts were immunoprecipitated with a primary antibody (2 μg/ml) at 4 °C for 4 h. Immunoprecipitates were washed twice with kinase reaction buffer (50 mM HEPES (pH 7.5), 10 mM MgCl2, 1 mM dithiothreitol, 2.5 mM EGTA, 1 mM NaF, 0.1 mM Na3VO4 and 10 mM glycerophosphate) and resuspended in 20 μl of kinase reaction buffer. The kinase assay was initiated by adding 20 μl of kinase reaction buffer, containing 10 μg of substrate and 2 μCi of [32P]ATP (ICN). Reactions were performed at 30 °C for 30 min, and terminated by adding SDS sample buffer. Mixtures were boiled for 5 min. The reaction products were analyzed by SDS-PAGE and autoradiography.

Clonogenic survival assay in soft agar. Rat2 fibroblast cells (1×10^4 cells) were suspended in 2 ml of 0.3% Difco Noble agar (Difco, Detroit, MI, USA) supplemented with complete culture medium. This suspension was layered over 2 ml of 0.8% agar medium base layer in 60-mm dishes and followed by incubation for 14 days at 37 °C in 5% CO2 incubator. Before counting colonies, the culture medium was decanted and the cells were fixed in 95% methanol and stained with 0.5% crystal violet. The numbers of colonies (>50 cells) from triplicate dishes were counted. Mean colony numbers relative to control colony numbers were plotted.

Tumor formation in xenograft mice. Rat2 fibroblast cells (1×10^7 cells) were trypsinized, washed with PBS and suspended in 100 μl PBS. A 100 μl of cell suspension was injected subcutaneously into each nude mouse (BALB/c, male). The growth of these tumors was monitored by two-day intervals, and growth rates were determined using caliper measurements. Tumor volume was calculated according to the following equation: tumor volume (g) = (length (mm) $\times$ width (mm)^2) $\times$ 0.5. Experiments were terminated 21–31 days after tumor cell injection. Each group was given injections with Rat2 fibroblast cells infected or transfected with retroviral K-Ras, retroviral DN-p38, DN-PKCδ, catalase, MFG empty vector and PCDNA empty vector.

Rac GTP exchange assay. Cell lysates were prepared for the Rac1 Activation Assay (Upstate Technologies, Lake Placid, NY, USA). Briefly, cells were lysed in magnesium lysis buffer (MLB) supplemented with 10 μg/ml leupeptin, 10 μg/ml apoprotin, 1 mM sodium vanadate and 1 mM sodium fluoride. Cell lysates were precleared for 10 min with GST beads and then incubated with PAK-1 PBD agarose beads for 1 h at 4 °C. Beads were washed three times in MLB and then 1 × SDS loading dye was added to the beads for electrophoresis. The samples were boiled for 5 min and resolved by 12% SDS-PAGE. Proteins were transferred to a nitrocellulose membrane and GTP-bound Rac1 was identified with an anti-Rac1 antibody.

Measurement of ROS generation. Briefly, cells (2×10^5 cells) were infected with K-Ras^{V12} for the indicated times. After infection, cells were incubated in 10 μM DCFDA (Molecular Probes, Eugene, OR, USA) at 37 °C for 30 min, and harvested by trypsinization and washed with cold PBS solution three times. ROS were determined by FACS analysis or after incubation with 10 μM DCFDA, the cells were immediately observed under a confocal laser-scanning microscope (Leica; Leica Microsystems, Wetzlar, Germany).

Plasmid construction. The DNA fragments encoding the full length of p47^{phox} (amino acid 1–390), PX domain of p47^{phox} (amino acid 1–125), SH3-N domain of p47^{phox} (amino acid 156–215), SH3-C domain of p47^{phox} (amino acid 226–285) and PP domain of p47^{phox} (amino acid 292–390), and the full length of PKCδ were amplified from cloned cDNAs encoding human p47^{phox} and PKCδ by PCR using specific primers, and then ligated to pCMV-HA (Clontech, Palo Alto, CA, USA), for the full length of p47^{phox} and PKCδ, to pFLAG-CMV2 (Sigma-Aldrich Co) for PX, SH3-N, SH3-C and PP domains, and to pGEX-2T (Amersham Biosciences, Piscataway, NJ) for the full length of p47^{phox}, PX, SH3-N, SH3-C and PP domains, and the full length of PKCδ. Ser345, Ser348, Ser359, Ser370, Ser379, Ser348/379 and Ser345/359 on p47^{phox}, and Tyr311, Thr505, Tyr523 and Tyr565 on PKCδ were mutated to alanine using the site-directed mutagenesis kit (Clontech), and the mutated fragments of p47^{phox} and PKCδ were cloned into pGEX-2T and pCMV-HA vectors, respectively.

Expression of recombinant proteins. E. Coli strain BL21 (Invitrogen, San Diego, CA, USA) was transformed with pGEX-2T-p47^{phox}, pGEX-2T-PX, pGEX-2T-SH3-N, pGEX-2T-SH3-C, pGEX-2T-PP, pGEX-2T-p47^{phox} (S345A), pGEX-2T-p47^{phox} (S348A), pGEX-2T-p47^{phox} (S359A), pGEX-2T-p47^{phox} (S370A), pGEX-2T-p47^{phox} (S379A), pGEX-2T-p47^{phox} (S348/379A) or pGEX-2T-p47^{phox} (S345/359A). GST-fusion proteins were purified by glutathione-sepharose (Amersham), according to the manufacturer's protocols. Purified GST-fusion proteins were stored in PBS containing 0.5 mM DTT and 0.2 mM PMSF at 4 °C.

p47^{phox} GST pull-down assay. A total of 10 μl of glutathione-sepharose beads coupled to GST, GST-p47^{phox}, GST-PX, GST-SH-N, GST-SH-C or GST-PP were incubated with 300 μl of cell lysate at 4 °C overnight. Following incubation, beads were washed five times with cell lysis buffer, and bound proteins were resolved by SDS-PAGE and detected by western blot analysis.

***In vitro* kinase assay.** 0.5 μg of wild-type GST-p47^{phox}, GST-p47^{phox} (S345A), GST-p47^{phox} (S348A), GST-p47^{phox} (S359A), GST-p47^{phox} (S370A), GST-p47^{phox} (S379A), GST-p47^{phox} (S348/379A) and GST-p47^{phox} (S345/359A) were, respectively, incubated with 0.5 μg of active PKCδ (Upstate Biotechnology Inc.) in 20 μl of kinase buffer (50 mM HEPES (pH 7.5), 10 mM MgCl2, 1 mM dithiothreitol, 2.5 mM EGTA, 1 mM NaF, 0.1 mM Na3VO4 and 10 mM glycerophosphate) containing 2 μCi of [32P]ATP (ICN) for 30 min at 30 °C. Reactions were terminated by adding 2 × SDS sample buffer. Mixtures were boiled for 5 min. The reaction products were analyzed by SDS-PAGE and autoradiography.

RT-PCR. Total RNA was prepared from Rat2 fibroblast cells using Trizol reagent (Gibco Invitrogen Corp), according to the manufacturer's protocols. TAKARA reverse-transcriptase-PCR kit (Takara Bio Inc., Otsu, Shiga, Japan) was used for cDNA synthesis. PCR reactions were performed with oligonucleotides (listed below) composed of targeted Rat cDNA sequences. The following primers were used for PCR; Rat Nox1, 5′-AGCCATTGGATCACAACCTC-3′ (sense), 5′-TAGGGACTCCTGCAACTCCT-3′ (antisense); Rat Nox2, 5′-TCCTTCGTGGTT GCTCTCTT-3′ (sense), 5′-GCTTATCACAGCCACAAGCA-3′ (antisense); Rat Nox3, 5′-TGGATAGTGGGTCCCATGTT-3′ (sense), 5′-CAGGTGATAACGCTCCA GCT-3′ (antisense); Rat Nox4, 5′-TGTCTGCTTGTTTGGCTGTC-3′ (sense), 5′-CTGAGAAGTTCAGGGCGTTC-3′ (antisense); Rat NOXO-1, 5′-CCTTCTCTGT GTGCTGGTCA-3′ (sense), 5′-TTGGCCTGTTGCTATCTCCT-3′ (antisense); Rat p47^{phox}, 5′-CCACCTCCTCGACTTCTTCA-3′ (sense), 5′-CCGAGGTCTTCTCGTA GTCG-3′ (antisense); Rat GAPDH, 5′-ATGGGAAGCTGGTCATCAAC-3′ (sense), 5′-TTCACACCCATCACAAGCAT-3′ (antisense).

Conflict of Interest

The authors declare no conflict of interest.

Acknowledgements. This work was supported by the National Research Foundation (NRF) and Ministry of Science, ICT and Future Planning, Korean government, through its National Nuclear Technology Program (2012M2A2A7035878 and 2012M2B2B1055639).

1. Sundaresan M, Yu ZX, Ferrans VJ, Irani K, Finkel T. Requirement for generation of H2O2 for platelet-derived growth factor signal transduction. *Science* 1995; **270**: 296–299.
2. Bae YS, Kang SW, Seo MS, Baines IC, Tekle E, Chock PB *et al.* Epidermal growth factor (EGF)-induced generation of hydrogen peroxide. Role in EGF receptor-mediated tyrosine phosphorylation. *J Biol Chem* 1997; **272**: 217–221.
3. Leto TL, Geiszt M. Role of Nox family NADPH oxidases in host defense. *Antioxid Redox Signal* 2006; **8**: 1549–1561.
4. Thannickal VJ, Fanburg BL. Reactive oxygen species in cell signaling. *Am J Physiol Lung Cell Mol Physiol* 2000; **279**: L1005–L1028.
5. Orient A, Donko A, Szabo A, Leto TL, Geiszt M. Novel sources of reactive oxygen species in the human body. *Nephrol Dial Transplant* 2007; **22**: 1281–1288.
6. Halliwell B, Gutteridge JM, Cross CE. Free radicals, antioxidants, and human disease: where are we now? *J Lab Clin Med* 1992; **119**: 598–620.
7. Cross CE, Halliwell B, Borish ET, Pryor WA, Ames BN, Saul RL *et al.* Oxygen radicals and human disease. *Ann Intern Med* 1987; **107**: 526–545.
8. Kim C, Kim JY, Kim JH. Cytosolic phospholipase A(2), lipoxygenase metabolites, and reactive oxygen species. *BMB Rep* 2008; **41**: 555–559.
9. Vafa O, Wade M, Kern S, Beeche M, Pandita TK, Hampton GM *et al.* c-Myc can induce DNA damage, increase reactive oxygen species, and mitigate p53 function: a mechanism for oncogene-induced genetic instability. *Mol Cell* 2002; **9**: 1031–1044.
10. Gianni D, Taulet N, DerMardirossian C, Bokoch GM. c-Src-mediated phosphorylation of NoxA1 and Tks4 induces the reactive oxygen species (ROS)-dependent formation of functional invadopodia in human colon cancer cells. *Mol Biol Cell* 2010; **21**: 4287–4298.
11. Ferro E, Goitre L, Retta SF, Trabalzini L. The interplay between ROS and Ras GTPases: physiological and pathological implications. *J Signal Transduct* 2012; **2012**: 365769.
12. Yang JQ, Li S, Huang Y, Zhang HJ, Domann FE, Buettner GR *et al.* V-Ha-Ras overexpression induces superoxide production and alters levels of primary antioxidant enzymes. *Antioxid Redox Signal* 2001; **3**: 697–709.
13. Bos JL. ras oncogenes in human cancer: a review. *Cancer Res* 1989; **49**: 4682–4689.
14. Adjei AA. Blocking oncogenic Ras signaling for cancer therapy. *J Natl Cancer Inst* 2001; **93**: 1062–1074.
15. Yang JQ, Li S, Domann FE, Buettner GR, Oberley LW. Superoxide generation in v-Ha-ras-transduced human keratinocyte HaCaT cells. *Mol Carcinog* 1999; **26**: 180–188.
16. Yang JQ, Buettner GR, Domann FE, Li Q, Engelhardt JF, Weydert CD *et al.* v-Ha-ras mitogenic signaling through superoxide and derived reactive oxygen species. *Mol Carcinog* 2002; **33**: 206–218.
17. Cullen JJ, Weydert C, Hinkhouse MM, Ritchie J, Domann FE, Spitz D *et al.* The role of manganese superoxide dismutase in the growth of pancreatic adenocarcinoma. *Cancer Res* 2003; **63**: 1297–1303.
18. Ang KK, Peters LJ, Weber RS, Morrison WH, Frankenthaler RA, Garden AS *et al.* Postoperative radiotherapy for cutaneous melanoma of the head and neck region. *Int J Radiat Oncol Biol Phys* 1994; **30**: 795–798.
19. Maciag A, Sithanandam G, Anderson LM. Mutant K-rasV12 increases COX-2, peroxides and DNA damage in lung cells. *Carcinogenesis* 2004; **25**: 2231–2237.
20. Ralph SJ, Rodriguez-Enriquez S, Neuzil J, Saavedra E, Moreno-Sanchez R. The causes of cancer revisited: 'mitochondrial malignancy' and ROS-induced oncogenic transformation—why mitochondria are targets for cancer therapy. *Mol Aspects Med* 2010; **31**: 145–170.
21. Mitsushita J, Lambeth JD, Kamata T. The superoxide-generating oxidase Nox1 is functionally required for Ras oncogene transformation. *Cancer Res* 2004; **64**: 3580–3585.
22. Cheng G, Lambeth JD. NOXO1, regulation of lipid binding, localization, and activation of Nox1 by the Phox homology (PX) domain. *J Biol Chem* 2004; **279**: 4737–4742.
23. Ago T, Kuribayashi F, Hiroaki H, Takeya R, Ito T, Kohda D *et al.* Phosphorylation of p47phox directs phox homology domain from SH3 domain toward phosphoinositides, leading to phagocyte NADPH oxidase activation. *Proc Natl Acad Sci USA* 2003; **100**: 4474–4479.
24. Yuzawa S, Suzuki NN, Fujioka Y, Ogura K, Sumimoto H, Inagaki F. A molecular mechanism for autoinhibition of the tandem SH3 domains of p47phox, the regulatory subunit of the phagocyte NADPH oxidase. *Genes Cells* 2004; **9**: 443–456.

25. Symonds JM, Ohm AM, Carter CJ, Heasley LE, Boyle TA, Franklin WA *et al.* Protein kinase C delta is a downstream effector of oncogenic K-ras in lung tumors. *Cancer Res* 2011; **71**: 2087–2097.
26. Pylayeva-Gupta Y, Grabocka E, Bar-Sagi D. RAS oncogenes: weaving a tumorigenic web. *Nat Rev Cancer* 2011; **11**: 761–774.
27. Avruch J, Khokhlatchev A, Kyriakis JM, Luo Z, Tzivion G, Vavvas D *et al.* Ras activation of the Raf kinase: tyrosine kinase recruitment of the MAP kinase cascade. *Recent Prog Horm Res* 2001; **56**: 127–155.
28. Welman A, Griffiths JR, Whetton AD, Dive C. Protein kinase C delta is phosphorylated on five novel Ser/Thr sites following inducible overexpression in human colorectal cancer cells. *Protein Sci* 2007; **16**: 2711–2715.
29. Parekh DB, Ziegler W, Parker PJ. Multiple pathways control protein kinase C phosphorylation. *Embo J* 2000; **19**: 496–503.
30. Stephens L, Anderson K, Stokoe D, Erdjument-Bromage H, Painter GF, Holmes AB *et al.* Protein kinase B kinases that mediate phosphatidylinositol 3,4,5-trisphosphate-dependent activation of protein kinase B. *Science* 1998; **279**: 710–714.
31. Alessi DR, James SR, Downes CP, Holmes AB, Gaffney PR, Reese CB *et al.* Characterization of a 3-phosphoinositide-dependent protein kinase which phosphorylates and activates protein kinase Balpha. *Curr Biol* 1997; **7**: 261–269.
32. Stokoe D, Stephens LR, Copeland T, Gaffney PR, Reese CB, Painter GF *et al.* Dual role of phosphatidylinositol-3,4,5-trisphosphate in the activation of protein kinase B. *Science* 1997; **277**: 567–570.
33. Le Good JA, Ziegler WH, Parekh DB, Alessi DR, Cohen P, Parker PJ. Protein kinase C isotypes controlled by phosphoinositide 3-kinase through the protein kinase PDK1. *Science* 1998; **281**: 2042–2045.
34. Hata K, Ito T, Takeshige K, Sumimoto H. Anionic amphiphile-independent activation of the phagocyte NADPH oxidase in a cell-free system by p47phox and p67phox, both in C terminally truncated forms. Implication for regulatory Src homology 3 domain-mediated interactions. *J Biol Chem* 1998; **273**: 4232–4236.
35. Nitti M, Furfaro AL, Cevasco C, Traverso N, Marinari UM, Pronzato MA *et al.* PKC delta and NADPH oxidase in retinoic acid-induced neuroblastoma cell differentiation. *Cell Signal* 2010; **22**: 828–835.
36. Nitti M, Furfaro AL, Traverso N, Odetti P, Storace D, Cottalasso D *et al.* PKC delta and NADPH oxidase in AGE-induced neuronal death. *Neurosci Lett* 2007; **416**: 261–265.
37. Cai W, Torreggiani M, Zhu L, Chen X, He JC, Striker GE *et al.* AGER1 regulates endothelial cell NADPH oxidase-dependent oxidant stress via PKC-delta: implications for vascular disease. *AmJ Physiol Cell Physiol* 2010; **298**: C624–C634.
38. Raimondi C, Falasca M. Targeting PDK1 in cancer. *Curr Med Chem* 2011; **18**: 2763–2769.
39. Xie Z, Yuan H, Yin Y, Zeng X, Bai R, Glazer RI. 3-phosphoinositide-dependent protein kinase-1 (PDK1) promotes invasion and activation of matrix metalloproteinases. *BMC Cancer* 2006; **6**: 77.
40. Eser S, Reiff N, Messer M, Seidler B, Gottschalk K, Dobler M *et al.* Selective requirement of PI3K/PDK1 signaling for Kras oncogene-driven pancreatic cell plasticity and cancer. *Cancer Cell* 2013; **23**: 406–420.
41. Aoki Y, Niihori T, Narumi Y, Kure S, Matsubara Y. The RAS/MAPK syndromes: novel roles of the RAS pathway in human genetic disorders. *Hum Mutat* 2008; **29**: 992–1006.
42. Molina JR, Adjei AA. The Ras/Raf/MAPK pathway. *J Thorac Oncol* 2006; **1**: 7–9.
43. Kim RK, Suh Y, Lim EJ, Yoo KC, Lee GH, Cui YH *et al.* A novel 2-pyrone derivative, BHP, impedes oncogenic KRAS-driven malignant progression in breast cancer. *Cancer Lett* 2013; **337**: 49–57.

Supplementary Information accompanies this paper on Cell Death and Differentiation website (http://www.nature.com/cdd)